




# Screening Current Induced Field Changes During De-Energization With Axial Clamping

D. Kolb-Bond , M. D. Bird , Senior Member, IEEE, T. Painter , Sanath K. Ramakrishna, and Arneil Reyes

**Abstract**—The Screening Current Induced Field (SCIF) is useful to determine the gross field contribution of screening currents in a superconducting coil, specifically coils wound with large aspect ratio, single filament high temperature superconductors (HTS) such as Rare Earth Barium Copper Oxide (REBCO). Our numerical model accurately predicted the behavior of the SCIF shape and magnitude during energizing to full field but diverged on de-energization. We suggest that axial clamping and its associated consequences at high field are responsible for the difference in the computed SCIF upon de-energization. Simple methods of approximating this effect and comparisons between numerical and measurement results are presented.

**Index Terms**—Electromagnetic fields, magnetic hysteresis, numerical analysis, screening currents, solenoids.

## I. INTRODUCTION

SCREENING currents and their effect on superconductors [1], [2] and superconducting magnets has been an important topic for some time. Screening Current Induced Field (SCIF) has been a useful measurement in the development of computation models that calculate screening currents in REBCO magnets [3]–[12]. Defined as the difference between the field including screening currents and field without, it is a representation of the macro contribution of all present screening currents on the magnetic field. It is typically presented at the central field of a solenoid ( $B_z(0,0)$ ) where a magnet gets its quoted field. Many groups have calculated, measured, and compared the SCIF at low with great success. The other important consequence of screening currents is the strain associated, which has been calculated [12]–[21]. At higher field, the SCIF (and strain from screening currents (SCS)) did not agree as well, implying a difference in the screening currents distribution as higher fields were reached. It was suggested that the tilting of the conductor could improve agreement and was demonstrated with a simple approximation. [15] Recently, groups have included this tilt effect using a coupled electromagnetic and structural model

Manuscript received November 30, 2021; revised January 31, 2022 and February 23, 2022; accepted March 15, 2022. Date of publication March 24, 2022; date of current version May 6, 2022. This work was performed at the National High Magnetic Field Laboratory which is supported in part by NSF cooperative agreement DMR-1644779 and in part by the State of Florida. (Corresponding author: D. Kolb-Bond.)

D. Kolb-Bond, M.D. Bird, and T. Painter are with the National High Magnetic Laboratory, Tallahassee, FL 32310 USA, and also with Florida State University, Tallahassee, FL 32306 USA (e-mail: kolb-bond@asc.magnet.fsu.edu).

Sanath K. Ramakrishna and Arneil Reyes are with the National High Magnetic Laboratory, Tallahassee FL 32310 USA.

Color versions of one or more figures in this article are available at <https://doi.org/10.1109/TASC.2022.3162162>.

Digital Object Identifier 10.1109/TASC.2022.3162162

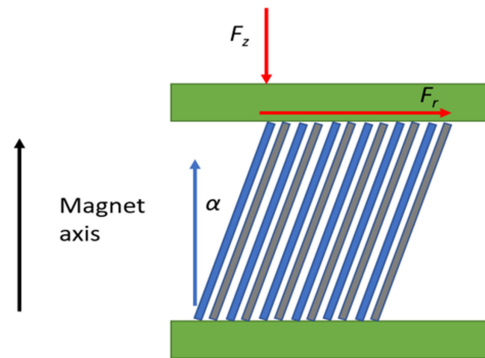


Fig. 1. Diagram showing rotation angle, axial force and the friction “clamping” force. Conductor, cowind, and pancake spacers shown in blue, grey, and green respectively.

capable of iteratively computing screening current distributions and rotation angles at every timestep [20], [21]. These models show improved agreement in SCS and SCIF. However, a difference exists in the SCIF hysteresis on de-energizing the coil to zero field. In a high field coil the axial force can be enormous and it was hypothesized that an axial “clamping” force that generates radial friction between pancake spacers and pancake windings could slow or prevent movement on ramping down (Fig. 1) This effect was approximated by decoupling the structural model from the electromagnetic and including the rotation angle in the equations without the displacement dependence. By forcing a rotation angle, we can modify the behavior without having to model complicated structural mechanics. Cases are considered and compared with measurement.

## II. ANALYTICAL METHOD

The “coupled” electromagnetic and structural model calculates a local rotation angle as a function of the change in radial displacement with respect to the magnet axis ( $\alpha = du/dz$ ) using a structural mechanics model and applies it to the electromagnetic equations governing screening currents [20], [21]. This rotation has marked changes on the normal field induction and critical current respectively shown in (3) and (4) because of changes to the normal and parallel field in (1) and (2). With reasonable justification the rotation angle can be decoupled from the structural mechanics and included as a function of time without any dependence on displacement. Using our “coupled” model “FloSSS” [20] we had calculated the maximum rotation angle in the windings of 32 T HTS coils (Table I) when ramped

TABLE I  
COIL PARAMETERS

Coil Parameters	Coil 1	Coil 2
IR, OR [mm]	20, 70	82, 116
Turns	254	150
Half-height [mm]	90	162
$I_{op}$	173	173

TABLE II  
 $I_c$  PARAMETERS

$I_c$ Parameters	VALUES
$I_{c0}$ [A]	2896
$k$	0.00913
$\mu$	0.7518
$B_0$	0.4674

to full field. We take the calculated rotation angles from that analysis and include them as a normalized function of time i.e., completely removing the structural mechanics model and any rotation angle dependence on displacement or Lorentz force. The analysis is thus much closer to energizing a coil and manually rotating each turn. This decoupling allows us to modify the behavior of the rotation angle and observe its effect on the SCIF. The goal being to slow down the rotation on de-energization to simulate a “clamping”. We first look at a single pancake in 32 T coil 1 (Pancake #8 from midplane) to observe whether our method would have meaningful effect on the SCIF behavior before moving to a “full-scale” calculation with all pancakes in both coils (112 total pancakes) and comparing with measurement. Coil parameters used for the 32 T All Superconducting Magnet and  $I_c$  fit parameters are shown in Tables I and II respectively.

$$B_n = B_r \cos(\alpha) - B_z \sin(\alpha) \quad (1)$$

$$B_p = B_z \cos(\alpha) + B_r \sin(\alpha) \quad (2)$$

$$\frac{dB_n}{dt} = \left( \frac{dB_r}{dt} \cos(\alpha) - \frac{dB_z}{dt} \sin(\alpha) \right) - \frac{d\alpha}{dt} (B_r \sin(\alpha) + B_z \cos(\alpha)) \quad (3)$$

$$I_c = I_{c0} / \left( 1 + \frac{\sqrt{k^2 B_p^2 + B_n^2}}{B_0} \right)^{-\mu} \quad (4)$$

### III. CASE 1: SINGLE PANCAKE

In pancake #8 we calculated the max rotation angle to be  $4^\circ$  at full field. We apply a normalized rotation angle to the entire pancake (no radial dependence) and apply it as a function of time (Fig. 2) for three difference scenarios. This uniform rotation angle across the width of the pancake is closer to rigid body rotation than local bending and is most applicable in coils with self-supporting turns which is largely the case in the 32 T. The first scenario uses a linear ramp to full field and a linear

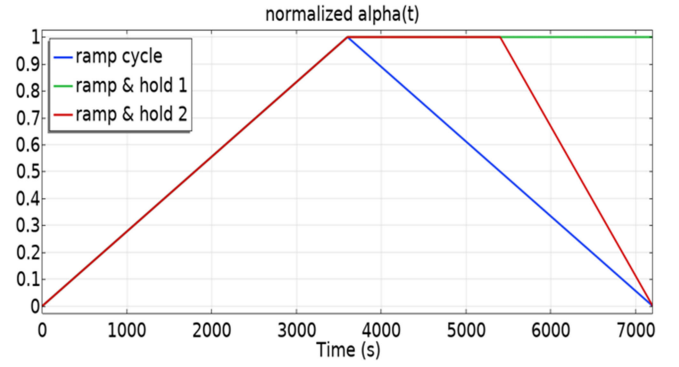


Fig. 2. Normalized rotation angle as a function of time. Blue: linear ramp up and down. Green: linear ramp up and hold for entire de-energization to simulate total clamping. Red: linear ramp up and hold for half of de-energization to simulate clamp and release.

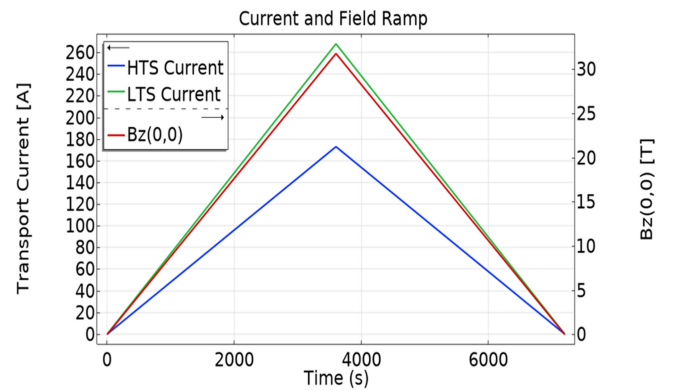


Fig. 3. Current and field energization profile for all rotation angle scenarios.

ramp back to zero. The second scenario “ramp & hold 1” uses a linear ramp to full field before holding at maximum for the entire de-energization to simulate “clamping” preventing the conductor from rotating back to its initial position i.e., static friction. The third scenario “ramp & hold 2” uses a linear ramp to full field before holding for half of the de-energization before linearly decreasing to zero. This scenario attempts to simulate a “clamped” for half of de-energization i.e., static to frictionless. For each scenario the entire coil system is cycled according to Fig. 3.

Results for all three scenarios are compared in Fig. 4. In scenario one “ramp cycle” the SCIF hysteresis is the smallest, returning along a similar path. In “ramp up & hold 1”, by holding the rotation at maximum the hysteresis opens on de-energization before returning to 0. In “ramp up & hold 2” the hysteresis is open for the entire de-energization process back to zero. This numerical experiment shows that a “clamping” or a rotation angle that is not allowed to freely rotate can be a catalyst for the hysteresis being open. Another difference is the SCIF returns to 0. We suggest that this could imply the conductor rotation angle is indeed “clamped” on the beginning of de-energization but does not return to a zero-rotation angle at zero energization. Previously results that do not include the “rotation effect” have shown a return to non-zero remnant field. However, by omitting the rotation angle you are inherently “clamping” the conductor

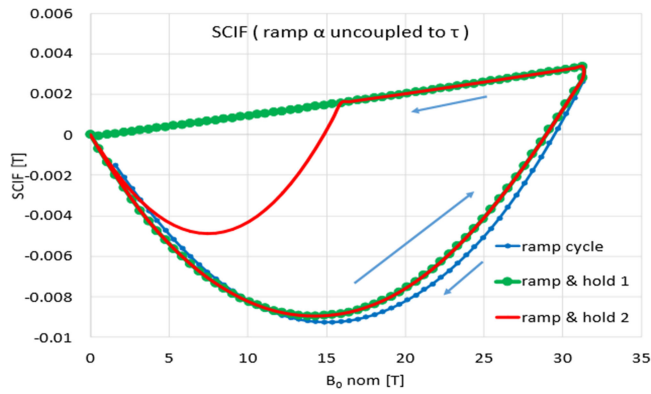


Fig. 4. SCIF plots for each scenario. Blue: linear ramp up and down. Green: linear ramp up and hold for entire de-energization to simulate total clamping. Red: linear ramp up and hold for half of de-energization to simulate clamp and release. Arrows showing direction of time.

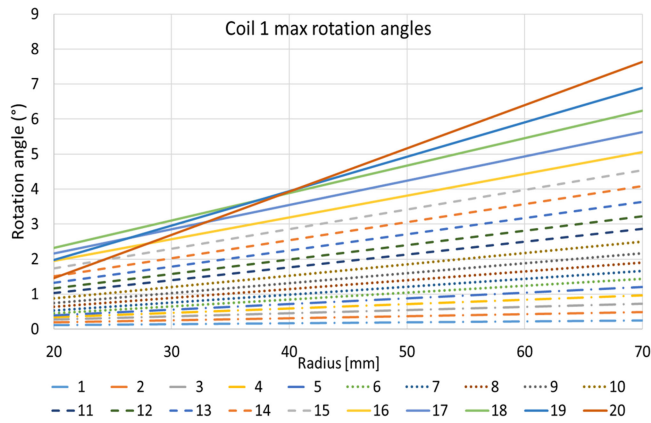


Fig. 5. Max rotation angle vs radius fits for each pancake (numbered from the midplane) of coil 1. Rotation angle at OD is monotonically increasing from the midplane to the end of the coil.

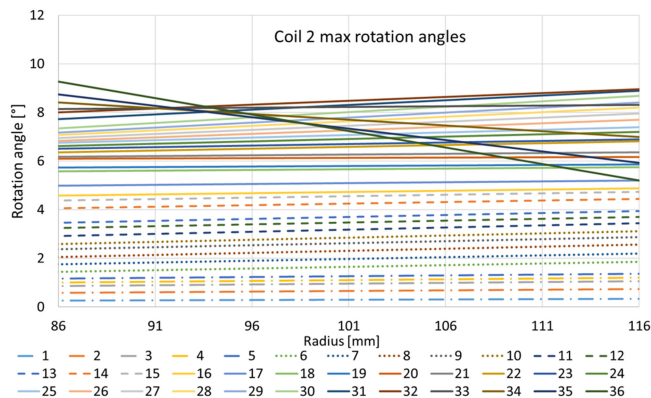


Fig. 6. Max rotation angle vs radius fits for each pancake (numbered from the midplane) of coil 2. Rotation angle at ID is monotonically increasing from midplane to the end of the coil.

by preventing its rotation (this is the same as forcing a rotation angle of zero throughout the entire energization cycle) increasing the negative screening current contribution at the edges. We include this in Case 2 when looking at all the pancakes in the 32 T. Last thing to note is that for all three scenarios the SCIF

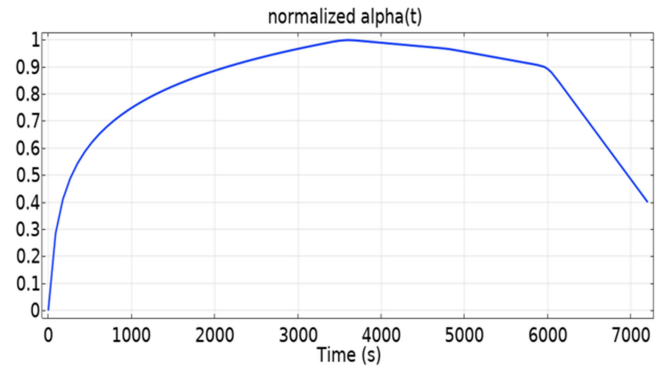


Fig. 7. Normalized rotation angle vs time used for all pancakes.

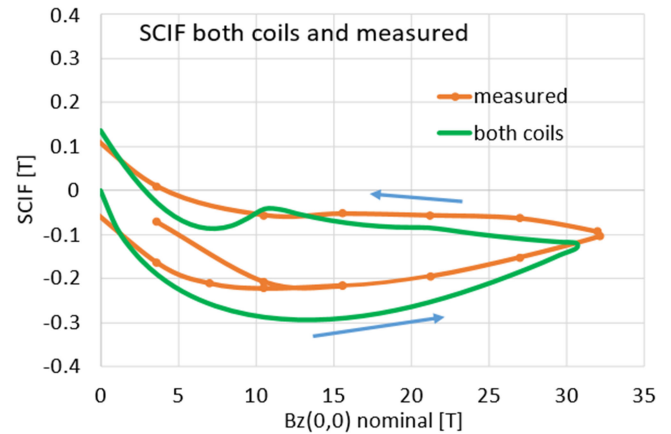


Fig. 8. Comparison of measured and computed values for central SCIF of the 32 T magnet vs. time. The measured values (orange) were previously presented in [20]. The measured data has been shifted down by 60 mT to adjust for the fact the magnet had been previously ramped prior to taking this measurement and had some trapped flux.

becomes positive near full field, this should only happen if the rotation angle is greater than the field angle generating screening currents in the opposite direction. This occurred because the field angle at the inner diameter (ID) of this coil is close to parallel with the magnet axis and thus using a uniform rotation angle for the entire pancake is not reasonable as we end up with sections of the pancake rotating past the magnetic field angle (generating negative screening currents and positive central field SCIF) which should not occur in normal operation as shown in [20]. We account for this in case 2.

#### IV. CASE 2: ALL PANCAKES

To compare accurately with the NMR measurement of SCIF we must take the sum of the SCIF contribution of each pancake in the HTS coil system. Using a similar approach to Case 1 but correcting for the error in a uniform rotation angle as function of radius, we now take the maximum rotation angle at the inner diameter and outer diameter (OD) from [20] for each pancake, and use a linear fit between the two values Figs. 5 and 6 for coils 1 & 2 respectively.

The normalized rotation angle as a function of time is shown in Fig. 7. Here we use an exponential fit for the energization to full field and two linear fits to simulate a loose “clamping” (i.e., kinetic friction) and a return to a non-zero rotation angle.

The result for this calculation is compared with the NMR measurement shown in Fig. 8. Comparing hysteresis, we see that a similar effect of opening the hysteresis loop occurs on de-energization. Returning to zero field the SCIF ends at a positive and close magnitude to the measured.

## V. CONCLUSION

We have shown that a “clamping” effect can be responsible for the observed discrepancy in the hysteresis of the measured and computed SCIF. Our approach considered is simplistic and relies on approximations. If this effect is deemed important an investigation into accurate implementation is also desired. These implementations could include pancake spacers with contact elements between spacer and winding edges (computationally intensive), friction force applied at edges (kinetic only is simplistic and a static and kinetic friction model is nonlinear and perhaps best to use contact elements which can handle this). Another effect not accounted for is the distribution of axial force along the axial length of the coil with a minimum at the coil ends and maximum at the coil midplane while the rotation of the conductor usually follows the opposite behavior. This suggests far more “clamping” near the midplane of the coil than at the ends which should be included in an improved model. A byproduct is that any “clamping” i.e., friction, will exist on energization as well, limiting the rotation angle (and associated strain) more so near the midplane than the end.

The largest consequence of this analysis is the implication that the conductors do not return to their initial position on de-energization when “clamped” due to large axial forces. This effect might not be visible without a high field coil capable of producing these forces. This also implies that the second cycle does not begin in the same state as the first and subsequent cycles as well. Upon returning to zero field the magnetic clamping is low (neglecting any outside mechanical clamping preload), and the tilted conductors will have less axial pressure reacted through the length of the coil as a function of the distribution of tilt angles across the radius creating a possible loose section of the windings. This conductor movement and the side effects associated should be considered in the design of future high field coils.

## ACKNOWLEDGMENT

The authors would like to thank Ernesto Bosque, Iain Dixon, and Andy Gavrilin for their insight and vibrant discussions.

## REFERENCES

- [1] E. H. Brandt, “Thin superconductors in a perpendicular magnetic ac field: General formulation and strip geometry,” *Phys. Rev. B.*, vol. 49, no. 13, pp. 9024–9040, Apr. 1994.

- [2] E. H. Brandt, “Superconductors of finite thickness in a perpendicular magnetic field: Strips and slabs,” *Phys. Rev. B.*, vol. 54, no. 6, pp. 4246–4264, Aug. 1996.
- [3] N. Amemiya *et al.*, “Magnetic field generated by shielding current in high Tc superconducting coils for NMR magnets,” *Supercond. Sci. Technol.*, vol. 21, no. 9, Jun. 2008, Art. no. 095001.
- [4] Y. Yanagisawa *et al.*, “Magnitude of the screening field for YBCO coils,” *IEEE Trans. Appl. Supercond.*, vol. 21, no. 3, pp. 1640–1643, Jun. 2011.
- [5] F. Grilli, E. Pardo, A. Stenvall, D. N. Nguyen, W. Yuan, and F. Gömöry, “Computation of losses in HTS under the action of varying magnetic fields and currents,” *IEEE Trans. Appl.*, vol. 24, no. 1, pp. 78–110, Feb. 2014, Art. no. 8200433.
- [6] M. Zhang *et al.*, “Study of second-generation high-temperature superconducting magnets: The self-field screening effect,” *Supercond. Sci. Technol.*, vol. 27, no. 9, Aug. 2014, Art. no. 095010.
- [7] H. Ueda *et al.*, “Numerical simulation on magnetic field generated by screening current in 10-T-class REBCO coil,” *IEEE Trans. Appl. Supercond.*, vol. 26, no. 4, Jun. 2016, Art. no. 4701205.
- [8] E. Pardo, “Modeling of screening currents in coated conductor magnets containing up to 40,000 turns,” *Supercond. Sci. Technol.*, vol. 29, no. 8, Jun. 2016, Art. no. 085004.
- [9] J. Xia *et al.*, “Electromagnetic modeling of REBCO high field coils by the H-formulation,” *Supercond. Sci. Technol.*, vol. 28, no. 12, 2015, Art. no. 125004.
- [10] S. Noguchi, “A simple screening current-induced magnetic field estimation method for REBCO pancake coils,” *Supercond. Sci. Technol.*, vol. 32, no. 4, Mar. 2019, Art. no. 045007.
- [11] E. Berrospe-Juarez *et al.*, “Real-time simulation of large-scale HTS system: Multi-scale and homogeneous models using the T-A formulation,” *Supercond. Sci. Technol.*, vol. 32, no. 6, Art. no. 065003.
- [12] Y. Li *et al.*, “Magnetization and screening current in an 800-MHz (18.8-T) REBCO NMR insert magnet: Experimental results and numerical analysis,” *Supercond. Sci. Technol.*, vol. 32, no. 10, 2019, Art. no. 105007.
- [13] J. Xia *et al.*, “Stress and strain analysis of a REBCO high field coil based on the distribution of shielding current,” *Supercond. Sci. Technol.*, vol. 32, no. 9, Jul. 2019, Art. no. 095005.
- [14] D. Kolb-Bond *et al.*, “Computing strains due to screening currents in REBCO magnets,” *IEEE Trans. Appl. Supercond.*, vol. 30, no. 4, Jun. 2020, Art. no. 4602805.
- [15] Y. Li *et al.*, “Screening-current-induced strain gradient on REBCO conductor: An experimental and analytical study with small coils wound with monofilament and striated multifilament REBCO tapes,” *IEEE Trans. Appl. Supercond.*, vol. 30, no. 4, Jun. 2020, Art. no. 4702305.
- [16] S. Takahashi *et al.*, “Hoop stress modification, stress hysteresis and degradation of a REBCO coil due to the screening current under external magnetic field cycling,” *IEEE Trans. Appl. Supercond.*, vol. 30, no. 4, Jun. 2020, Art. no. 4602607.
- [17] Y. Yan *et al.*, “Screening current effect on the stress and strain distribution in REBCO high-field magnets: Experimental verification and numerical analysis,” *Supercond. Sci. Technol.*, vol. 33, no. 5, 2020, Art. no. 05LT02.
- [18] E. Berrospe-Juarez, F. Trillaud, V. M. R. Zermeño, F. Grilli, H. W. Weijers, and M. D. Bird, “Screening currents and hysteresis losses in the REBCO insert of the 32 T all-superconducting magnet using T-A homogeneous model,” *IEEE Trans. Appl. Supercond.*, vol. 30, no. 4, Jun. 2020, Art. no. 4600705.
- [19] W. D. Markiewicz *et al.*, “Design of a superconducting 32 T magnet with REBCO high field coils,” *IEEE Trans. Appl. Supercond.*, vol. 22, no. 3, 2012, Art. no. 4300704.
- [20] D. Kolb-Bond *et al.*, “Screening current rotation effects: SCIF and strain in REBCO magnets,” *Supercond. Sci. Technol.*, vol. 34, no. 9, 2021, Art. no. 095004.
- [21] Y. Yan *et al.*, “Screening-current-induced mechanical strains in REBCO insert coils,” *Supercond. Sci. Technol.*, vol. 34, no. 8, 2021, Art. no. 085012.